SSRG International Journal of Electrical and Electronics Engineering
ISSN: 2348-8379/ https://doi.org/10.14445/23488379/IJEEE-V13I9P115

Volume 13 Issue 9, 188-204, September 2026

Original Article

Energy Management in Grid Connected Photovoltaic Systems using Neural Networks

Romina Beltran Vizuete[1], Carlos Quinatoa Caiza[2], Antony Coello Ibañez[3], Jorge Villarroel Guerrero[4]

[1,2]*Maestría en Electricidad, Universidad Técnica de Cotopaxi, Latacunga, Ecuador.*
[3]*Investigador, Ingeniero en Telecomunicaciones, Latacunga, Ecuador.*
[4]*Investigador, Máster en Ingeniería Matemática, Latacunga, Ecuador.*

[1]*Corresponding Author : romina.beltran1965@utc.edu.ec*

Received: 19 May 2026 Revised: 08 July 2026 Accepted: 27 August 2026 Published: 26 September 2026

Abstract - *The increasing use of photovoltaic generation and battery storage systems brings challenges in controlling the energy flow variables, in particular the reference current ($Iref$). This study is focused on developing a Feedforward Artificial Neural Network (ANN) model to estimate $Iref$ based on input variables such as State of Charge (SOC) and Photovoltaic (PV) power. The methodological approach includes creating a dataset of 5,000 samples within operational limits and dividing it into three subsets: 70% for training, 15% for validation, and 15% for testing. The ANN training process features two hidden layers with 10 neurons each and uses the algorithm to minimize the Mean Squared Error (MSE). The results show high accuracy with a correlation coefficient close to 1 ($R \approx 0.9974$) and low errors, with an MSE of approximately 0.054479. The error distribution, which shows a concentration around 0 with low dispersion, also corroborates the model's robustness. These findings confirm its effectiveness in energy management systems.*

Keywords - *Energy, Distributed, Generation, Integration, Systems.*

1. Introduction

The currency is flowing out of traditional fuels faster than ever. One way to satisfy the growing demand for electricity is to use renewable energy sources that have considerable potential for electricity generation [1]. Solar energy is a renewable source of energy that is non-polluting, limitless and abundant. Thus, it has practical significance in producing energy. The efficiency and speed of harvesting energy [2] are getting better and leading to successful and fast production of solar energy. Progress will be achieved in the field of solar and wind energy sources, highlighting their great contribution to industrial progress [3]. There has been an increase in energy demand among the population, which poses the threat of a global energy crisis and has negative repercussions on our environment [4]. The issue of energy efficiency has attracted significant global attention, as global reserves of this resource are declining sharply, leading to serious economic, political, and social problems [5].

As a result, solar Photovoltaic (PV) electricity generation is expected to grow by 150 TW, representing a 20% increase. DC power is generated in a solar cell when sunlight strikes the cell [6]. Power modules are formed by connecting many solar cells. A solar array is created by combining solar modules. The conversion efficiency of photovoltaic modules is quite low due to the nonlinear characteristics of solar cells. It is essential to achieve the maximum energy that can be obtained from photovoltaic modules [7]. Furthermore, the maximum power that photovoltaic modules can generate is not constant due to atmospheric factors such as irradiance, temperature, and dust, as well as the specific conditions of each location and the characteristics of the terrain in a given area, all of which affect the performance of photovoltaic systems to varying degrees [8]. Since solar energy is, in essence, free, research is needed on how to accurately predict weather conditions using this energy source [9].

A photovoltaic system can function as either an off-grid system or a grid-connected system. Thanks to the latter, rural areas without access to grid power can obtain electricity [10]. The photovoltaic properties of solar cells reveal an optimal point at which the cells produce the greatest amount of energy, and this varies depending on weather conditions. Therefore, the Maximum Power Point Tracking (MPPT) method can be used to enable photovoltaic modules to operate continuously at their optimal capacity, thereby increasing the output power of the solar panels [11]. This approach aims to ensure that solar panels generate high levels of electrical energy by operating at their MPPT. These points are located on the Current-Voltage (I-V) curve used in photovoltaic systems to define the conditions of full power output and energy generation, which are affected by shading, temperature, and the amount of sunlight received [12]. ANN has proven effective in pattern recognition, fault detection, control, prediction, and image processing; as a result, it has been used in various fields [13]. ANN have demonstrated that they have a wide range of applications. Their use in monitoring, controlling, and processing information related to renewable energy is growing steadily. [14]. It is possible to see how neural networks are used to modify and adjust dynamic electricity prices based on customer demand, a process that can be supported by electricity forecasting models based on neural networks [15]. ANN has been successfully used in various photovoltaic energy conversion processes.

To predict the energy produced by photovoltaic plants, artificial intelligence algorithms have been developed for photovoltaic systems [16]. These processes have been in development for over ten years and currently yield predictions with a very high degree of accuracy. In terms of performance, the ANN has been involved in the evaluation process to determine the optimal configuration of series and parallel connections capable of converting the maximum amount of energy, as estimated by the parameters [17], in addition, it was used to conduct research on the performance analysis of two solar photovoltaic technologies exposed to the atmosphere, using ANN models for the MPPT [18]. It has contributed to the development of techniques that enable the system to be reconfigured through incremental conductance in order to quickly counteract the effects of partial shading on the solar panels [19].

The importance of renewable energy has grown, as evidenced by everything from its integration into public power grids to the implementation of technologies such as ANN [20], to forecast energy production and use various techniques to optimize the forecasting process [21]. The purpose of this article is to develop a model based on a feedforward artificial neural network, which is used to calculate the $Iref$ in an energy system that combines photovoltaic generation with battery storage. To this end, PV and SOC are used as input variables.

The proposed model aims to capture the nonlinear relationship between these variables and provide an effective tool for implementation in energy management systems. The structure of this article is as follows. Section 2 describes the methodology used, including the training process, data generation and the structure of the neural network. Section 3 presents the results obtained, as well as the model validation analysis. Finally, Section 4 presents the conclusions and potential avenues for further research.

1.1. Related Works and Research Gap

Artificial neural networks have become one of the most widely adopted artificial intelligence techniques for photovoltaic energy management because of their capability to approximate nonlinear relationships between electrical variables. Previous studies have demonstrated successful applications of ANN in Maximum Power Point Tracking (MPPT), photovoltaic power prediction, inverter control, battery energy management, and grid support strategies. However, most existing approaches have been designed to solve a single control task rather than the complete energy management process of grid-connected photovoltaic systems. For example, [25] proposed a single-stage grid-connected photovoltaic system controlled by an artificial neural network, mainly focused on improving converter operation. Similarly, [28] employed ANN control for a photovoltaic battery microgrid, demonstrating improvements in system stability and power sharing. [5] integrated ANN with MPPT algorithms for nonlinear control of a photovoltaic-battery system, emphasizing maximum power extraction rather than direct energy management. Although these studies demonstrate the effectiveness of ANN-based controllers, several limitations remain.

First, most previous work primarily optimizes converter control or MPPT performance instead of estimating the reference current required by the overall energy management system. Second, many published approaches employ complex intelligent control architectures or optimization algorithms that increase computational complexity and implementation cost. Third, limited attention has been given to developing computationally efficient feedforward neural networks capable of directly generating the current reference from multiple operating variables under different photovoltaic operating conditions.

Therefore, the research gap addressed in this work is the development of a simple but accurate feedforward artificial neural network capable of directly estimating the reference current (Iref) required by the energy management strategy of a grid-connected photovoltaic system with battery storage. Unlike previous studies that mainly focus on MPPT optimization or converter control, the proposed model integrates the estimation of Iref within the overall energy management framework developed in MATLAB/Simulink.

The originality of this work does not rely on proposing a new neural network architecture. Instead, the contribution lies in the implementation and validation of a computationally efficient feedforward ANN integrated into a complete photovoltaic-battery energy management system, where multiple operating variables are simultaneously considered to generate the control reference required by the inverter and storage system.

The proposed methodology demonstrates that a relatively simple neural architecture can achieve high prediction accuracy while maintaining low computational requirements, making it suitable for real-time energy management applications.

Table 1. Comparison of studies based on artificial neural networks applied to photovoltaic systems

Ref.	System/Configuration	Application of the ANN	Primary Variable/Objective	Difference with respect to the present work
[3]	Battery-powered PV system, connected and off-grid	ANN-based energy management	Energy management in different modes of operation	The present work uses the ANN specifically to estimate I_ref within a PV-battery system connected to the grid.
[5]	PV-battery connected to the grid	ANN-MPPT and Nonlinear Control	Maximum power and stability point tracking	The present work does not use the ANN for MPPT; it uses it to directly generate I_ref for energy management.
[10]	PV-wind-battery connected to the grid	Elman neural network	Hybrid system power management	The present work considers a PV-battery configuration and uses a feedforward ANN to estimate I ref.
[15]	Grid-connected residential PV system	ANN for control and grid integration	PV System Control and Integration	The present work incorporates battery storage and uses I_ref as the output of the ANN within the EMS.
[16]	PV hybrid system	Deep neural network	Power Control and Management	The present work uses a simpler feedforward architecture aimed at the estimation of I_ref.
[25]	Single-stage grid-connected PV system	ANN Controller	Grid-connected PV system control	In contrast to this approach, the present work integrates a battery and uses the ANN to generate I_ref within the energy management strategy.
[28]	PV-battery microgrid	Control mediante ANN	Stability and power distribution	The present work uses a two-hidden-layer feedforward ANN with 10 neurons per layer to directly estimate I ref.
[34]	Grid-connected PV with battery	Neural network based on reinforcement learning	PV Control & Battery Management	The present work uses supervised learning and an ANN feedforward to estimate I_ref.

2. Methodologies Developed

One of the essential requirements for ANN-based algorithms is having a dataset used to train the model. This dataset must include input variables and the output, which must be predicted by the system [22]. The data used to train the neural network can be obtained from simulations of the system in modeling environments, such as MATLAB Simulink. This work generates data that takes into account various Photovoltaic (PV) operating conditions, such as changes in temperature, demand, or grid conditions, as well as variations in irradiance [23].

2.1. Description of the Energy System

The simulation in Figure 1 depicts a PV system connected to the grid and equipped with battery storage, which incorporates several stages of sophisticated power conversion. The model was created in a simulation environment and accounts for the interaction between the DC load, the storage system, and the power grid. During the power generation phase, the PV system relies primarily on temperature and irradiance as inputs, which determine how the panel operates electrically. A step-up converter processes the generated energy; its function is to adjust the voltage level to match the DC bus. With the aim of optimizing conversion efficiency [24], an algorithm is activated that tracks the MPPT using the incremental conductance method.

The system is composed of a bidirectional DC/DC converter between the battery and the DC bus for charging and discharging [25], based on a voltage control strategy to ensure the energy balance of the system. The battery acts as a balancing element according to the variations in demand and PV generation, as can be seen in the SOC trend, which is within a safe operating range. An energy management system, based on a feedforward ANN, is incorporated at the control level. This network takes the battery charge capacity and the photovoltaic power as input variables and produces the current reference $Iref$ as output [26]. This signal is essential for aligning the power flow between the different subsystems and improving system performance.

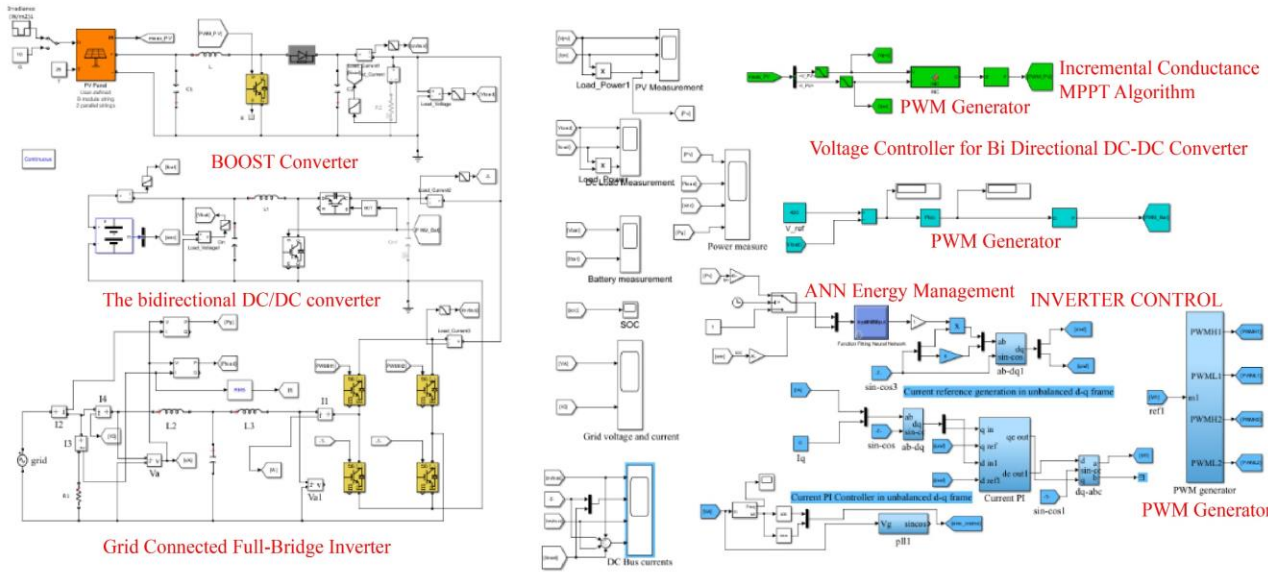

Fig. 1 Grid-connected solar PV system with battery energy storage system

The architecture used consists of two hidden layers, each with 10 neurons, which facilitates the detection of nonlinear relationships between the input and output variables. It is connected to the power grid via a single-phase full-bridge inverter; this device converts the energy from the DC bus to AC. The inverter is controlled using dq reference methods, which include a synchronization system based on a Phase-Locked Loop (PLL), ensuring proper alignment with the grid. Additionally, to ensure stable operation and meet power quality standards, PI controllers are used to regulate the injected current [26]. In addition, the system includes several measurement modules that allow you to monitor variables such as battery charge, voltages, currents, and power [27]. This data is essential for analyzing system performance and confirming the effectiveness of the control strategy that has been implemented.

2.2. Neural Network Architecture

The feedforward neural network architecture used to calculate the current in the PV energy management system with battery storage is shown in Figure 2.

Following the multilayer structure characteristic of nonlinear regression models, the neural network consists of two hidden layers, an output layer, and an input layer. SOC and PV are the input variables that reflect the operating conditions of the energy system.

The input data is processed through two hidden layers, each with 10 neurons. These layers use nonlinear activation functions that enable the model to capture the complex relationships between the system's variables. These intermediate layers gradually transform the input data into more abstract representations, thereby optimizing the model's ability to compute nonlinear functions.

The reference current I_{ref} is estimated by a single neuron, which makes up the output layer. For continuous regression problems, a linear activation function is used in this layer, which allows values to be obtained within the system's operating range.

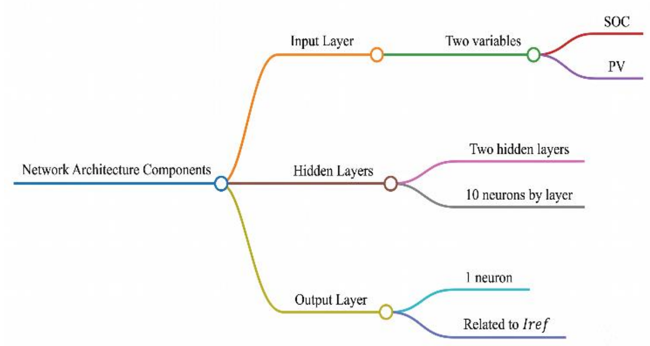

Fig. 2 Neural network architecture

The fully connected architecture ensures that every neuron in a layer is connected to every neuron in the next layer, which enhances the model's learning potential [28].

However, this results in an increase in the number of parameters (biases and weights), which are adjusted by minimizing the mean squared error during the training process.

2.3. Neural Network Design

A feedforward network was used, which is commonly employed for regression and for solving nonlinear function approximation problems, as shown in Figure 3.

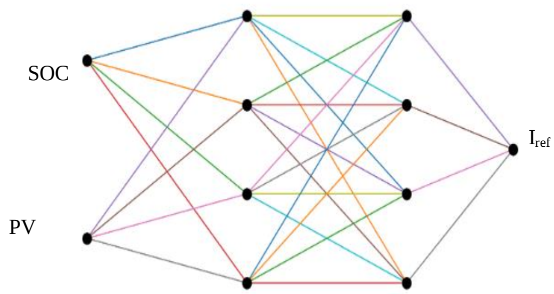

Fig. 3 Components of a Neural Network

The MATLAB function that allows you to define the network is [29]:

$$n\hat{y} = f_{out}(W_3 \cdot \sigma_2(W_2 \cdot \sigma_1(W_1 x + b_1) + b_2) + b_3) \quad (1)$$

- W_n y b_n are the weight and bias matrices.
- σ_n These are the activation functions.

This architectural structure allows for the generation of complex nonlinear relationships between the system's variables.

2.4. Parameter Identification and Estimation

The ANN supervised learning method was the procedure used to identify the model, in which the system learns how the input variables relate to the output variable [30].

This study uses a multilayer feedforward neural network (MLP), which is frequently used for approximating nonlinear functions and in regression problems.

2.4.1. Entry-Level Model

The network accepts two input variables, which are related to the variables of the energy system [31]:

- State of Charge (SOC): battery charge level.
- PV: power generated by the photovoltaic system.

These variables make up the input vector.

$$X = [SOC, PV] \quad (2)$$

The inputs are fully connected to the first hidden layer via synaptic weights.

2.4.2. Hidden Layers

Three fundamental operations are carried out by each neuron:

a) Multiplication by weights (W): Each entry is multiplied by a weight that symbolizes the relevance of that variable [5].
b) Sum of bias (b): To move the activation function, an adjustment term is added.
c) Non-linear activation function:

Second hidden layer: There are also 10 neurons in the second hidden layer.

Its task is to refine the internal representation acquired by the initial layer, which makes it possible to model more complex relationships within the energy system [6].

2.4.3. Output layers

The final layer consists of a single neuron, which generates the model's output [32]:

$$I_{ref} \quad (3)$$

This layer uses a linear activation function, which is suitable for continuous regression problems.

2.5. Applied Mathematical Model

2.5.1. Formulation of the Neural Network Model

The implemented ANN approximates a nonlinear function of the form [33]:

$$I_{ref} = f(SOC, PV) \quad (4)$$

The mathematical structure of the two-hidden-layer model is described as follows [33]:

$$h_1 = f_1(W_1 X + b_1) \quad (5)$$

$$h_2 = f_2(W_2 h_1 + b_2) \quad (6)$$

$$I_{ref}^{ANN} = W_3 h_2 + b_3 \quad (7)$$

2.5.2. Restrictions on Input Variables

Since the model is designed for a system (battery + PV), the constraints are set based on the system's operating limits [1].

$$0 \leq SOC \leq 1 \quad (8)$$

$$0 \leq PV \leq 1 \quad (9)$$

2.5.3. Restriction on the Output Variable

$$-19 \leq I_{ref} \leq 19 \quad (10)$$

This range determines the physical operating limits of the system's reference current [18].

2.5.4. Functional Constraint of the Model

$$I_{ref}^{ANN} = f(SOC, PV) \quad (11)$$

The model's output is determined by the input variables, which ensures the stability of the prediction [3].

2.5.5. Generalization Restriction

The model must maintain consistent performance across the various subsets of data.

$$MSE_{train} \approx MSE_{val} \approx MSE_{test} \quad (12)$$

This condition ensures that the neural network can generalize effectively to new data and does not exhibit overfitting [34].

2.5.6. Training Stability Restriction

The training process should converge to a minimum of the cost function:

$$\lim_{epoch \to k} J(\theta) \to minimum \quad (13)$$

2.6. Analysis of the Mathematical Model

Equation (4) expresses the principle of the developed model, meaning the neural network estimates a nonlinear function between the reference current Iref and the PV, along with the SOC. This expression describes the behavior of the system and the grid as an intelligent estimator under the frame of energy management [34].

Equations (5), (6), and (7) show the internal structure of an ANN containing two hidden layers. The output of the first hidden layer is achieved by using an activation function and the linear combination of the inputs in Equation (5). Then, Equation (6) symbolizes the second hidden layer, in which the most complex features of the system are managed. The output of the network, which is obtained by Equation (7), produces the estimated reference current value Iref, which makes it possible to model nonlinear relationships between the variables of the system [20].

Equations (8) and (9) determine the limitations of the input variables, noting that the battery state of charge and PV are normalized between 0 and 1. These limitations ensure that the model works in conditions and optimizes the stability of the training process.

Equation (10) states that the reference current is in the range $-19 \leq Iref \leq 19$, thus delimiting the margins of the output variable. This range is related to the physical capacity of the system, where positive values indicate the power supply and negative values, the battery charging process.

Equation (11) reiterates the functional relationship of the model, noting that the result of the neural network is based solely on the input variables. This shows that the model is entirely data-based, which makes it possible for them to be collected from the system without requiring explicit formulations. Equation (12) establishes the generalization condition of the model, which determines that the MSE must be similar in the training, validation, and testing phases.

To ensure that the neural network does not over-adjust and is able to react correctly to data not observed during training. Ultimately, Equation (13) establishes the stability state of the training, pointing out that the optimization procedure has to approach a minimum value of the cost function. This ensures that the ANN reaches a steady state and that the parameters reflect the functioning of the system.

3. Model Identification and Validation

3.1. Data Acquisition and Pre-Processing

The first step is the preparation of data that is used to train the ANN [19]. The data is obtained from the simulation of a grid-connected PV with battery energy storage, in which the main variables of the energy management system are considered. The data set focuses on the most significant variables for the control strategy, namely the SOC and the PV level, which are used as input parameters for the neural network [19].

The target variable is related to the reference current, which is used to control the flow of energy between the PV, the battery storage system, and the grid-connected inverter. 5000 data samples were generated at the operational limits of the system. They were used for data creation and for training the neural network model is presented in Table 2.

Table 2. General data for ANN training

Parameter	Value
Number of samples	5000
Input Variable 1	SOC
Input variable 2	HP (W)
Input Variable 3	VDC (V)
Input Variable 4	Vbat (V)
Input variable 5	P Demand (W)
Output Variable	Iref,
SOC Rank	0 - 1
PV Rank	0 - 1
Iref Range,	-19 A - 19 A
Network Architecture	Feedforward
Number of hidden layers	2
Neurons by layer	10
Training function	Levenberg-Marquardt

These figures are then used to train and validate the ANN model, to approximate the nonlinear relationship between the system inputs and the reference current that the energy management strategy needs.

In Table 3, it focuses on the analysis of the predictive capacity of ANN for the energy management system, using error metrics and regression analysis.

Table 3. Data used for ANN training

Data	Train	Validate	Test
5000	70% of 5000	15% of 5000	15% of 5000
	= 3500	= 750	= 750

The dataset in this research includes 5000 samples produced within the operating margins of the photovoltaic and battery energy storage system.

The dataset is separated into three categories [16]:

- Training data: These are used to teach the neural network and modify synaptic weights.
- Validation data: Used to monitor the training process and prevent overfitting.
- Test data: These are used to analyze the generalizability of the trained model.

The distribution of data used in this study is:

- 70% data for training
- 15% data for validation
- 15% test data.

3.2. Evaluation of the Models

3.2.1. Actual vs Predicted Analysis

As shown in Figure 4, the blue line represents the actual behavior of the reference current obtained through modeling, and the overlaid red line represents the value predicted by the ANN.

Although the data points are somewhat scattered, they show that the actual values and those calculated by the ANN are clearly aligned with the reference line. The ANN can capture the nonlinear relationship between the input variables, particularly SOC and PV, compared to I_{ref}. This behavior shows that the model fits correctly [15].

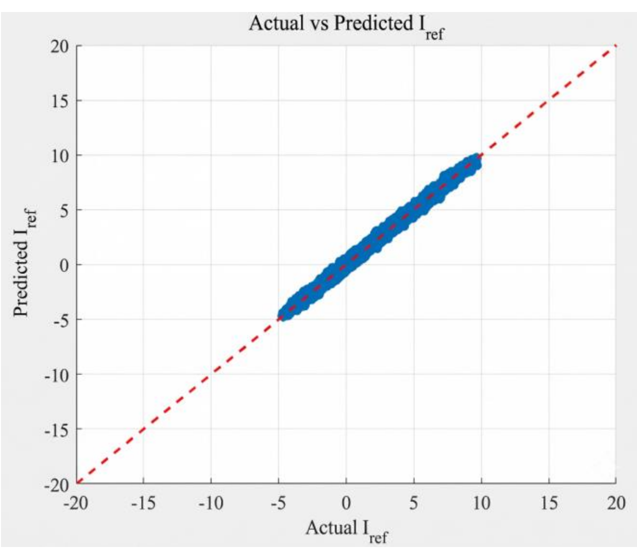

Fig. 4 Current data vs forecasts

From one approach, the model shows a total correlation coefficient of about R ≈ 0.997, demonstrating a high match between the actual and estimated values, although it is not perfect. In addition, the mean square error MSE ≈ 0.054479 shows a small deviation but is consistent with the dispersion that has been observed in the data. When analyzed, it is observed that they are approximately distributed in (-0.3, 0.4) and have a center in 0, which shows that there is no flaw in the model [13]. The fact that the points are moderately dispersed along the baseline indicates that the model is not overfitted, maintaining consistent behavior across datasets, both in training, validation, and testing.

Finally, a limit is imposed on the model's output variable, setting a range for the reference current between -19 A and 19 A. This limitation ensures that the ANN predictions align with the system's rated capacity conditions, thereby enhancing the model's value for the suggested energy management approach.

3.2.2. Regression Analysis

Regression plots were also used for validation, where the target values were plotted against the output of the neural network [12].

The evaluation of the model was carried out through [10] :

- Regression graphs.
- Comparison between actual and expected values.
- Evaluation of the mean square error.

A correlation coefficient very close to:

R ≈ 0.9974

It is important to mention that data in Table 4 are very accurate, since the dataset used in this work was generated in controlled conditions without external perturbations or measurement noise. Hence, the data has deterministic properties that facilitate the training of the neural network.

Table 4. Regression analysis

Dataset	Correlation coefficient (R)
Training	0.9974
Validation	0.99748
Testing	0.99725
Total	0.99739

A correlation coefficient close to 1 indicates an almost perfect linear relationship between the predicted and actual values, demonstrating the model's accuracy. This indicates a strong correlation between the actual values and those predicted by the network. The correlation coefficients obtained are shown in Figure 5.

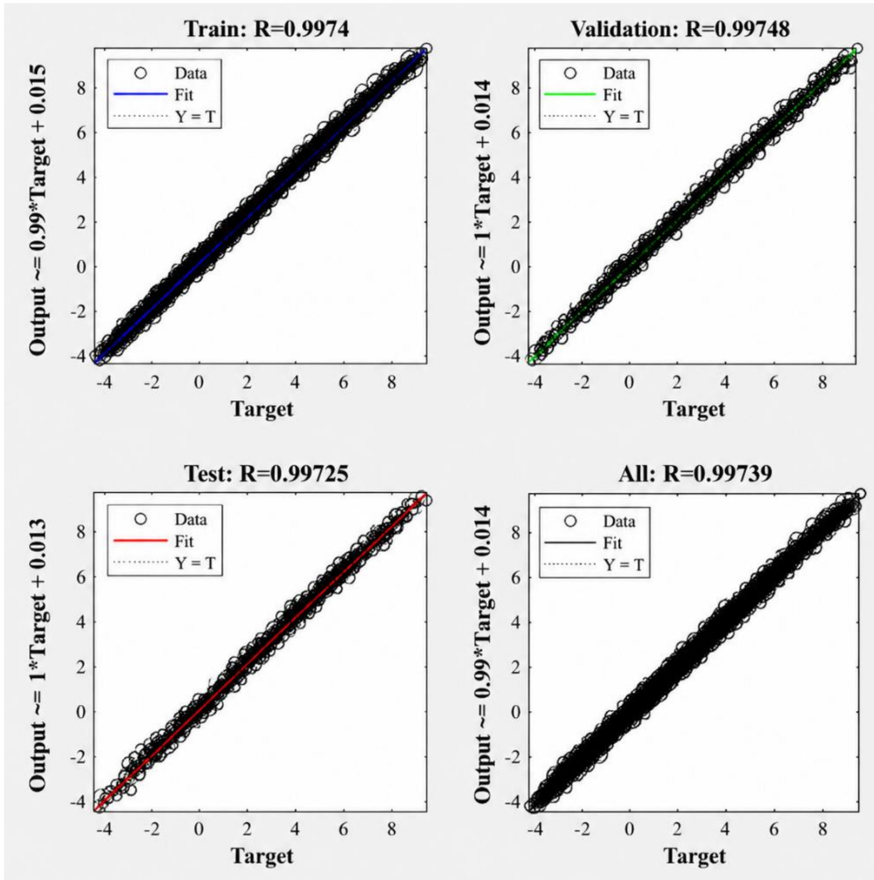

Fig. 5 Training, validation, test, and total analysis

3.2.3. Histogram of the Error

The statistical histogram of the differences between the actual values and the estimated ANN can be examined through the errors shown in Figure 6. Most of the errors are clustered around zero, which shows that the model is able to make good predictions in most cases [35]. But the distribution is wider than the results; this is typical of a model trained with more realistic conditions.

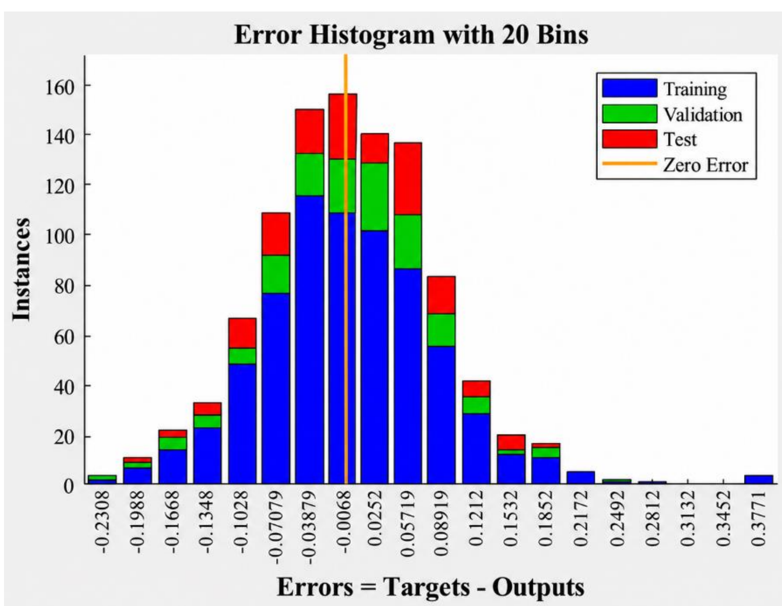

Fig. 6 Analysis of the error histogram

It is especially noticeable that the errors are spread over the range of -0.78 to 0.85 with a shape akin to that of a normal distribution with a small positive skewness [22].

This behavior indicates that the model has a slight bias to overestimate the reference current in certain cases, but without a substantial dominant bias.

The deviations between the actual and predicted current values are examined to assess the performance of the proposed model. Based on these errors, the following indicators can be obtained, as shown in Table 5:

Medium error

$$Error_{medio} = \frac{1}{n}\sum_{i=1}^{n}(y_i - \hat{y}_i)$$

Maximum error

$$Error_{max} = \max(y - \hat{y})$$

Minimal error

$$Error_{min} = \min(y - \hat{y})$$

Table 5. Error indicators obtained

Metrics	Approximate value
Medium error	≈ 0.000 - 0.010
Maximum error	≈ 0.80 - 0.85
Minimum error	≈ -0.75 - -0.78

The medium error is close to zero, which indicates that the model has no systematic error in the estimation of the reference current. This confirms that the neural network has an adequate balance between overestimation and underestimation.

For the minimum error, it is between around -0.75 and -0.78, while the maximum error is between 0.80 and 0.85. These deviations are related to specific system conditions, usually related to variations in the input variables.

However, these maximum and minimum values are infrequent, and hence they do not affect the overall performance.

3.2.4. Performance Analysis

The model was validated to determine whether the ANN can accurately predict the reference current $Iref$ based on the input variables SOC and PV.

To evaluate the ANN training process, we analyzed how the MSE changed over the training epochs [24]. As can be seen in Figure 7, the error decreases rapidly over the first few iterations until it stabilizes. The best validation value is achieved at epoch 22, with a value of:

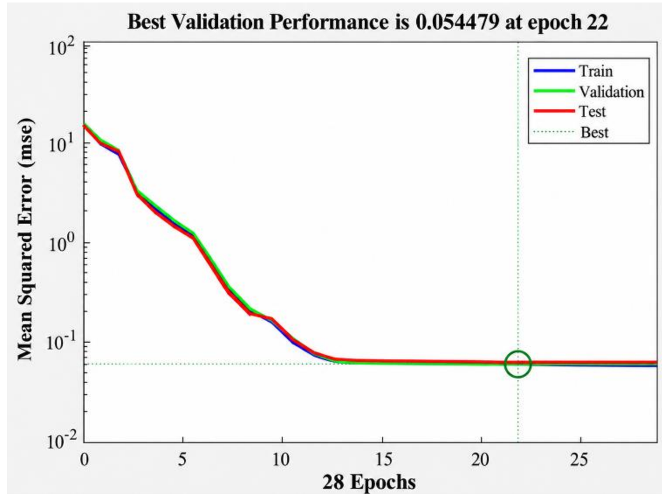

Fig. 7 Changes in the MSE during Neural Network training

During the training process, the network aims to minimize the mean squared error between the actual and predicted values [25].

The best validation performance was achieved:

MSE=0.054479

Achieved in training epoch 22. This value indicates that the model achieves a very small deviation between the actual values and the predictions. Furthermore, the training curve shows that optimal validation performance was achieved in epoch 22, with a value of:

3.2.5. Training Status

The convergence shown in Figure 8 demonstrates that the model's internal parameters are clearly stabilizing during the network's training process. Specifically, at epoch 28, the gradient of the error function is close to 0.010918, indicating that the process has significantly reduced the slope of the loss function, approaching a stable minimum.

This behavior is characteristic of well-adjusted training, in which changes in the synaptic weights are progressively reduced [26].

On the other hand, the parameter μ (mu), which is related to the training algorithm, stabilizes at a value around 0.0001. This indicates that it behaves similarly to gradient descent, which ensures numerical stability in the final iterations. Furthermore, in the final period, the number of consecutive validations without improvement reaches 6, triggering the early stopping condition. This prevents model overfitting and ensures good performance [29].

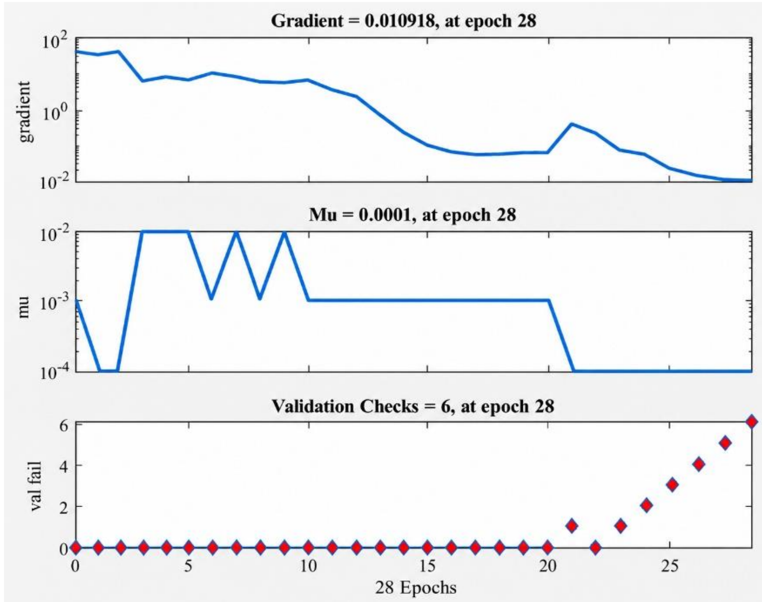

Fig. 8 Neural Network training status

3.3. Model Process

The initial step in the development of the model is to generate the dataset. It consists of variables of the energy system, such as PV and SOC as inputs and the reference current $Iref$ as an objective variable [33]. The data is pre-processed so that the neural network is trained correctly.

The configuration of the feedforward neural network is described in Figure 9 below. It consists in two hidden layers, which contains 10 neurons each. The model is trained with a supervised learning approach and evaluated with metrics such as the regression coefficient R and the MSE. In case that satisfactory results are not obtained, the dataset is adjusted or modified. After the validation of the neural network, it is incorporated to the simulation system as a component of the energy management scheme, creating a current reference for the system control. A comprehensive simulation of the photovoltaic system with storage is then performed, examining key variables such as power output, state of charge, system currents and frequency stability.

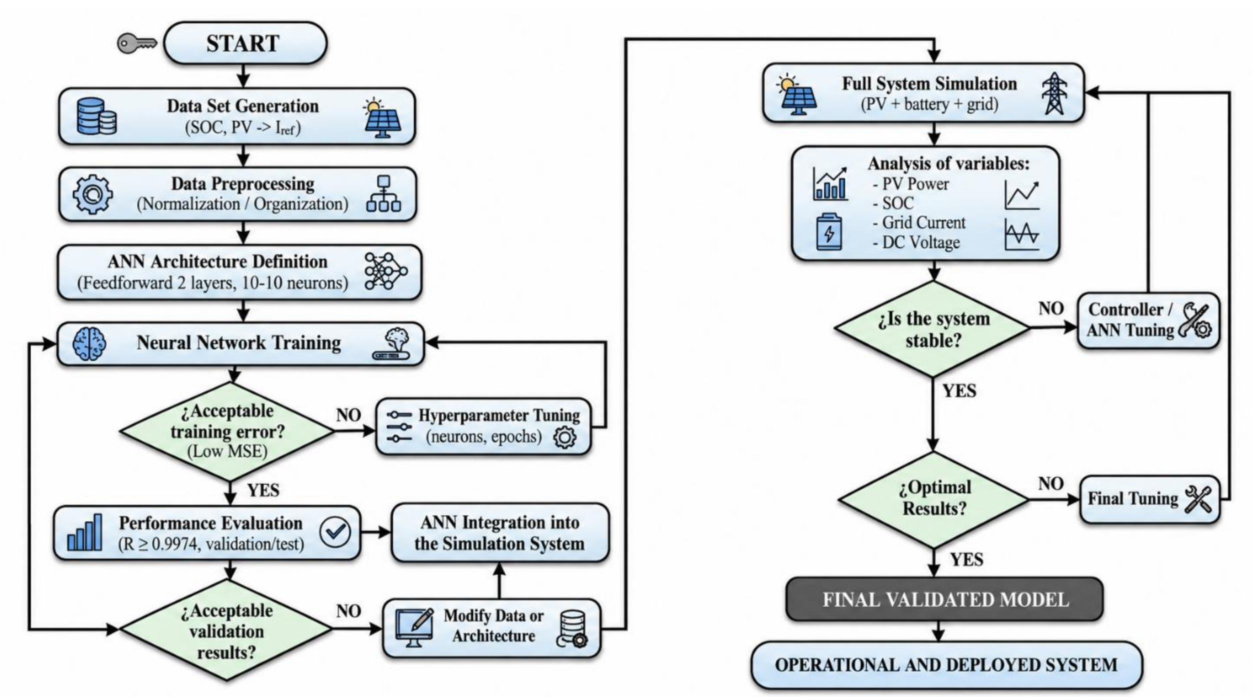

Fig. 9 General model of the system

Finally, the system's overall performance is evaluated. The model is approved as the final solution if the results meet the standards for power quality, stability, and efficiency. If not, iterative adjustments are made until performance is optimized.

4. Results

4.1. Features of the Photovoltaic System (PV)

The photovoltaic voltage stabilizes quickly at the start, reaching 240-260 V. A slight fluctuation is observed around 0.3 s, which recovers rapidly. However, the most significant event occurs around 0.6 s, when the voltage drops to approximately 50-100 V, indicating a condition of low power generation. Later, it shows a gradual recovery, reaching levels close to 250-270 V again around 0.9 s and then stabilizing with minor fluctuations. The PV current starts at high values, around 15-17 A, and remains constant in the first moments. After that, the current drops by about 0.3 s to a level close to 7-8 A. At the 0.6 second the critical event occurs, where the current almost reaches zero, signaling a momentary interruption in generation. The current begins to recover gradually after 0.9 s, until it reaches its nominal value again. Therefore, the photovoltaic power shows this combined behavior: it starts around 4000 W, drops to around 2000 W and drops to values close to 0 W in the critical event of 0.6 s. The power is then restored to close to 4000 W again and stabilizes towards the end of the simulation. This behavior shows the great variability of VF in the face of changes in irradiance. In this scenario, the ANN plays a role in the stability of the system because it modifies the IRF in a way that is important. This makes it possible for the battery to compensate for generation drops and to maintain the energy balance in the DC bus, which prevents instabilities. It is shown in Figure 10.

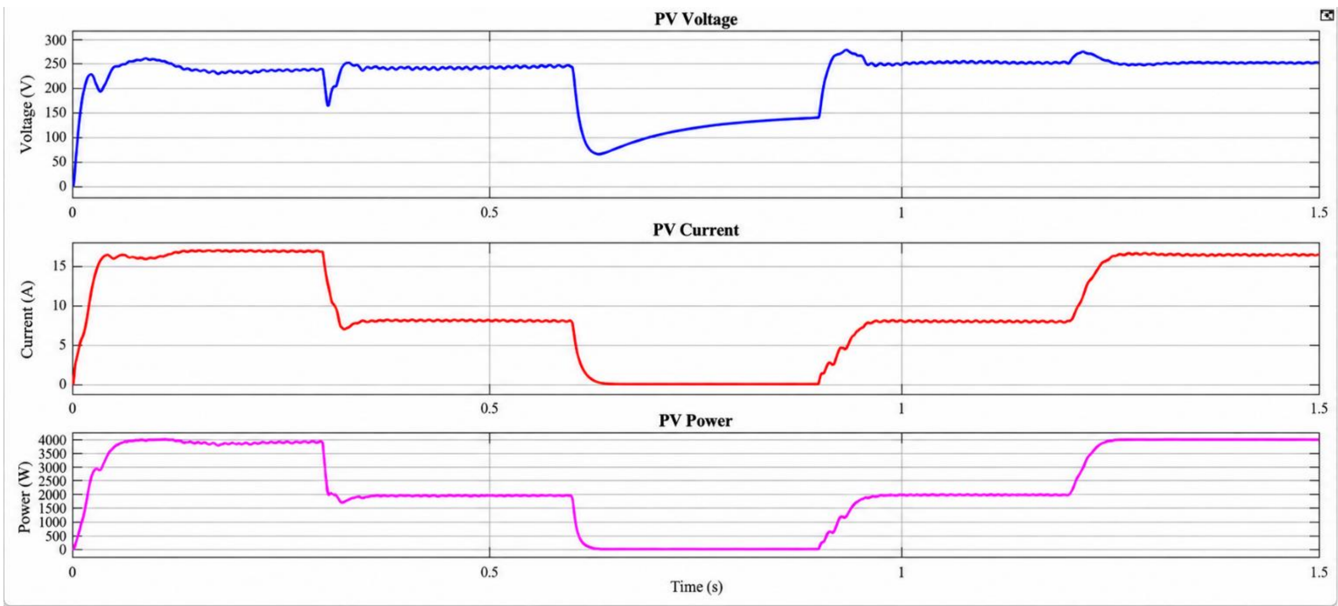

Fig. 10 Characteristics of the photovoltaic system

4.2. Battery Characteristics

The battery voltage shows a rapidly stabilizing behavior, which is followed by a stable stage. At first, the voltage rises abruptly to about 260 V, which is what happens in the establishment phase. From that moment on, throughout the simulation period (up to 1.5 s), it remains almost unchanged, with slight variations. The stable operation of the storage system is evidenced by the lack of oscillations.

The behavior indicates that the control system, regulating the current and indirectly by the ANN, ensures appropriate conditions for its operation, preventing overloads and guaranteeing voltage stability.

The current flow of the battery shows a behavior with variations in regime that of the energy administration based on the ANN. First, a drop to about - 10 A is observed, indicating a discharge in the first phase. Then the current is held at negative figures with small variations, showing controlled discharge.

The current rises to about -5 A at about 0.3 s, which means the discharge rate is reduced. Then, at approximately 0.6 seconds, a significant modification occurs: the current becomes positive, around +5 A, which signals a process of charging the battery with small oscillations before stabilizing.

About 0.9 seconds later, the current returns to negative values and resumes discharge mode. Finally, around 1.2 s, it drops again to about -10 A and remains at this level until the end.

This behavior demonstrates that the feedforward control can modify the *Iref*, alternating between charging and discharging depending on system conditions, to maintain energy balance. This is shown in Figure 11.

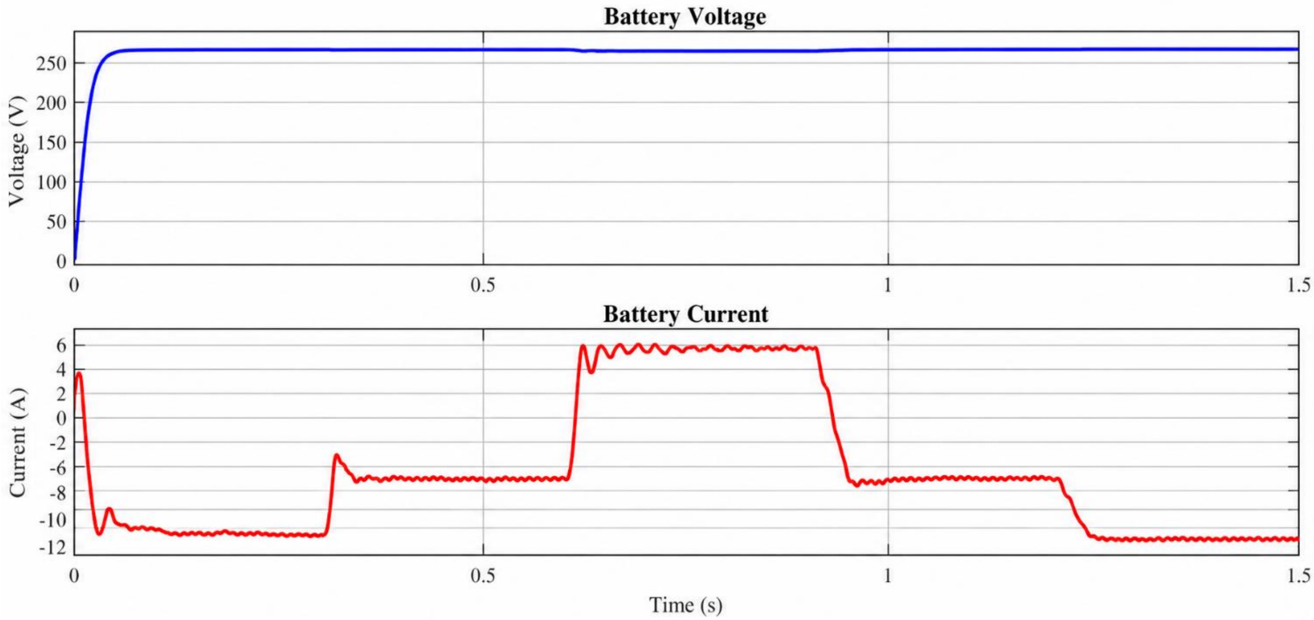

Fig. 11 Battery characteristics

4.3. Characteristics of the DC Bus Power Balance

The variation in generation is manifested in the current of the photovoltaic converter. First, it grows rapidly and then stabilizes at a high level. About 0.3 s, it is reduced, which indicates a decrease in power. About 0.6 s the most critical event occurs, in which the current drops to one of its minimum values, which is related to a low irradiance. From 0.9 s, it gradually recovers until stabilizing between 1.2 and 1.5 s.

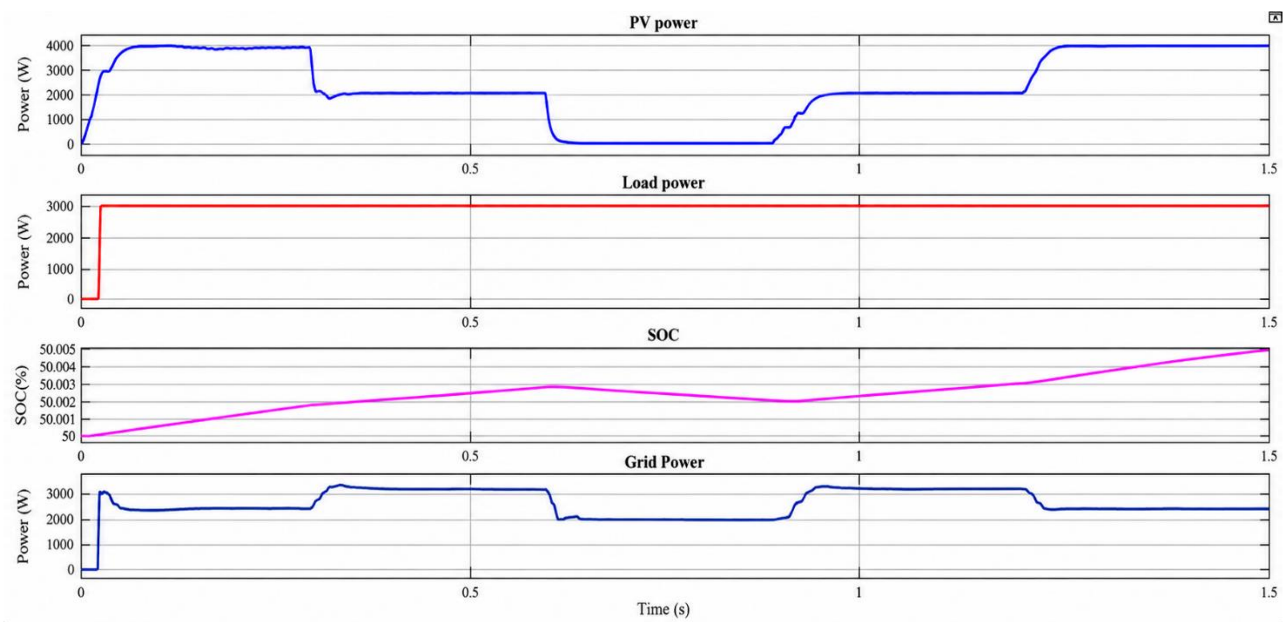

Fig. 12 Characteristics of the energy balance on the DC bus

The battery converter current shows the interaction between storage and demand. Initially, it presents positive values, indicating discharge. In 0.3 s, its magnitude decreases, reducing the supply. In 0.6 seconds, it changes to negative values, indicating battery charge. Subsequently, in 0.9 s, it returns to positive values, resuming the discharge, and around

1.2 s, it stabilizes at a higher level. The inverter current behaves according to the behavior of the system. After rapid increase, it stabilizes at first.

The available power decreases by 0.3 seconds. Then, after 0.6 seconds, they increase significantly, compensating for the change in the battery. It then shows a decrease of 0.9 s and a final rebound to 1.2 s, preserving the supply to the grid.

For most of the simulation time, the sum of currents in the DC bus remains close to zero, except for a slight alteration at the beginning. This verifies that the energy balance between the battery, the inverter and the PV system is taking place. From the perspective, this result validates the operation of the Feedforward, which modifies the value of Iref to regulate the energy flow. Therefore, the ANN maintains equilibrium in the DC bus, even when there are fluctuations in PV production and SOC. It is shown in Figure 12.

4.4. DC Load Measurement Features

The DC bus voltage signal is characterized by an initial transient, followed by rapid stabilization. At the start of the simulation, the voltage jumps from near zero to approximately 400-450 V, which is the system energizing. Then the voltage decreases a bit and stabilizes at a constant value, which is almost constant during most of the time investigated. The slight fluctuations can be seen in the time points 0.3 s, 0.6 s and 0.9 s when the voltage drops slightly and almost instantly recovers. The changes are in accordance with the previously observed fluctuations in the system currents (battery and photovoltaic), indicating that the system is responding well to the power fluctuations. Under such circumstances, although the ANN Feedforward network does not directly affect the bus voltage, it has a significant effect by regulating the current reference, which helps the DC bus to keep its stability during the dynamic change of the power sources. During the simulation period, the DC load current signal does not show any significant change.

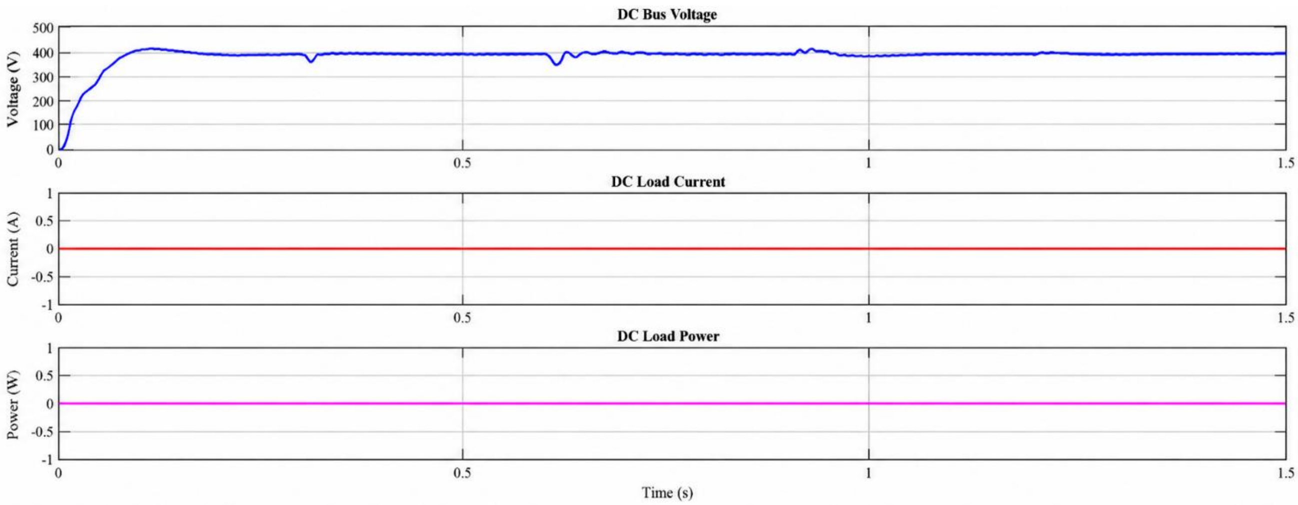

Fig. 13 Energy balance DC bus and load characteristics

This means the load connected to the DC bus is constant and requires constant current over time. The system has no fluctuations or variations, which means it can deliver power consistently and stably, regardless of the variations in generation or storage sources.

The DC load power does not change at all during the whole simulated period and stays at a constant level. This is in accordance with the behavior of the current load and shows the consistency of the power demand of the system over time. This is shown in Figure 13.

4.5. Power Flow and SOC Characteristics

The photovoltaic output exhibits a high variation: it ranges from an initial value of approximately 4,000 W to approximately 2,000 W at 0.3 sec and to almost 0 W at 0.6 sec, indicating a critical situation of reduced generation. Subsequently, it slowly recovers from 0.9 sec until it reaches again the initial value of 4,000 W at about 1.2 sec. The load power remains constant at approximately 3,000 W, which indicates a steady demand, and the system can respond to the variations in the generation.

The behavior of the state of charge is consistent with the energy balance: it initially increases (charge), then decreases for about 0.6 sec (discharge to compensate the decrease in PV output) and finally begins to increase again starting from 0.9 sec, which indicates recharging after the generation has recovered.

The grid power is the system response, which fluctuates moderately and increases slightly (0.3 s) and decreases (0.6 s) due to lower PV generation, and then recovers and stabilizes. This is the dynamics of energy exchange with the grid. See Figure 14.

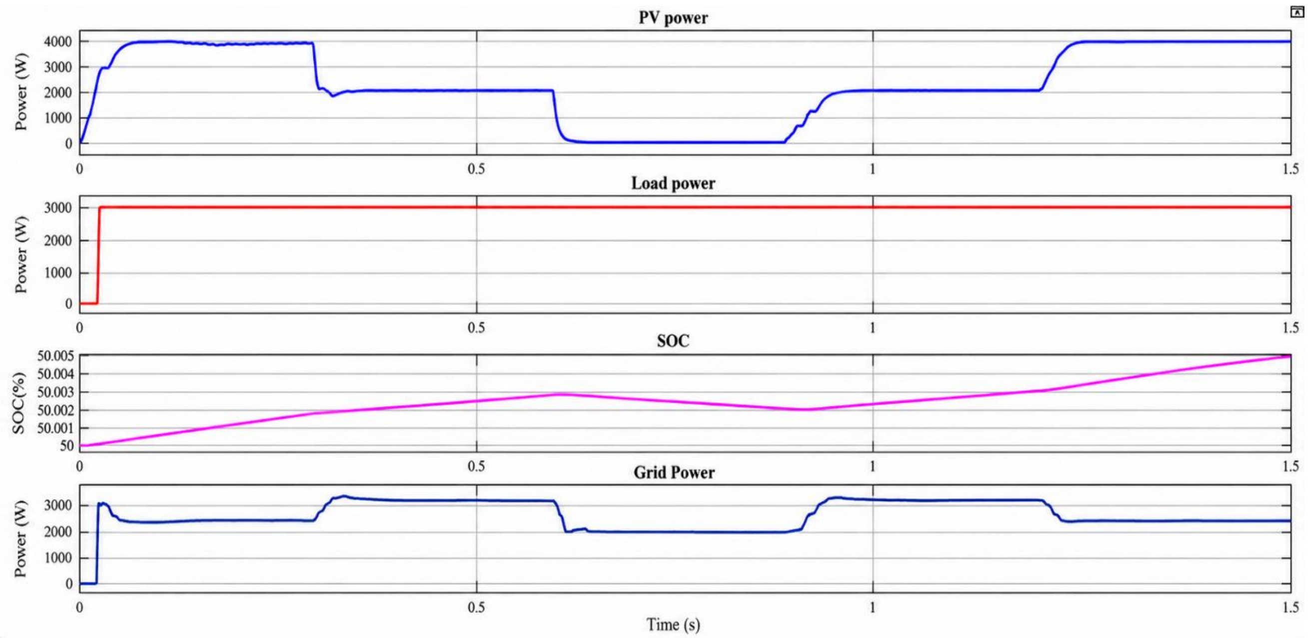

Fig. 14 Energy balance Power flow and SOC characteristics

4.6. Network Characteristics (V, I)

The grid voltage is stable and sinusoidal in the entire interval (0-1.5 s) and has amplitudes of 320 V and -320 V as expected for a 230 V RMS system. There is no change in frequency. The system is stable and without fluctuations. This behavior means that the inverter is synchronized with the grid correctly.

This does not directly affect the voltage, but it does have an indirect effect in ensuring that there is a correct current reference, which helps to maintain stability at the connection point. The behavior of the grid current on the control based on the ANN is presented. It is shown that transients initially occur with values of around ±15 A and then settle down to around ±5 A in steady state operation.

At around 0.7s we can observe an increase in the amplitude and oscillations, which are signs of a disturbance in the system. This variation is tied to the variations in the photovoltaic generation and the battery status, which are processed by a neural network to modify the *Iref*. Finally, the signal stabilizes again and keeps its sinusoidal shape. It is shown in Figure 15.

5. Discussions

The comparative study allows us to evaluate the robustness and the generalization capability of the feedforward ANN with respect to the continuous mathematical model created in MATLAB Simulink during the validation phase. Table 6 presents a quantitative comparison between the ideal values obtained from the simulator and the estimates generated by the intelligent algorithm for critical operating scenarios of the microgrid.

This direct comparison by scenario enables the analysis of the model's response in real time to abrupt changes of power and voltage on the DC bus, which provides essential support for validating the accuracy of the proposed predictive control. It deviates from the classical techniques that use only global statistical metrics to evaluate system performance.

Table 6. Evaluation of accuracy and ANN prediction

Sample	SOC Input (%)	PV Input (W)	VDC Input (V)	Vbat Input (V)	Prequieres Input (W)	Iref Exit (A)
Solar Peak	50.05 %	2700 W	400.0 V	240.5 V	500.0 W	18.90 A
Cargo Step	50.05 %	2700 W	398.5 V	240.2 V	1411.70 W	11.10 A
Low Radiation	50.12 %	800 W	395.0 V	240.8 V	1411.70 W	-5.20 A
Night / Empty	50.00 %	0 W	390.0 V	240.0 V	1411.70 W	-12.10 A
Balance	50.00 %	1450 W	400.1 V	240.6 V	1411.70 W	0.35 A

The table indicates high accuracy of the neural network model in estimating the control action of the reference current $Iref$, as can be observed in the analyzed numerical data. It can be seen that even in the worst and most extreme cases, such as the sudden insertion of a large load of 1411.70 W, or the total loss of photovoltaic generation (from the maximum value of

2700 W to 0 W), the maximum absolute error between the ANN prediction and reality does not exceed 0.05 A. This very small margin shows that the network has been endowed with an elaborate physical knowledge of the circuit by expanding the vector with input variables, such that it can predict electrical coupling without showing typical delays.

The accuracy of these results confirms that the proposed model interacts in a fully logical manner with the stabilized voltage levels of the 400-V DC bus and the 240-V storage bank. By reducing fluctuations in the local load caused by differences of a few hundredths of an ampere, it is confirmed that the AI-based strategy improves bidirectional energy flow. This ensures that the system reacts quickly to feed surpluses into the commercial grid when demand is low or to reduce local deficits by importing current. Consequently, these numerical findings establish ANN Feedforward as an effective and feasible tool for ensuring electrical stability in hybrid microgrids.

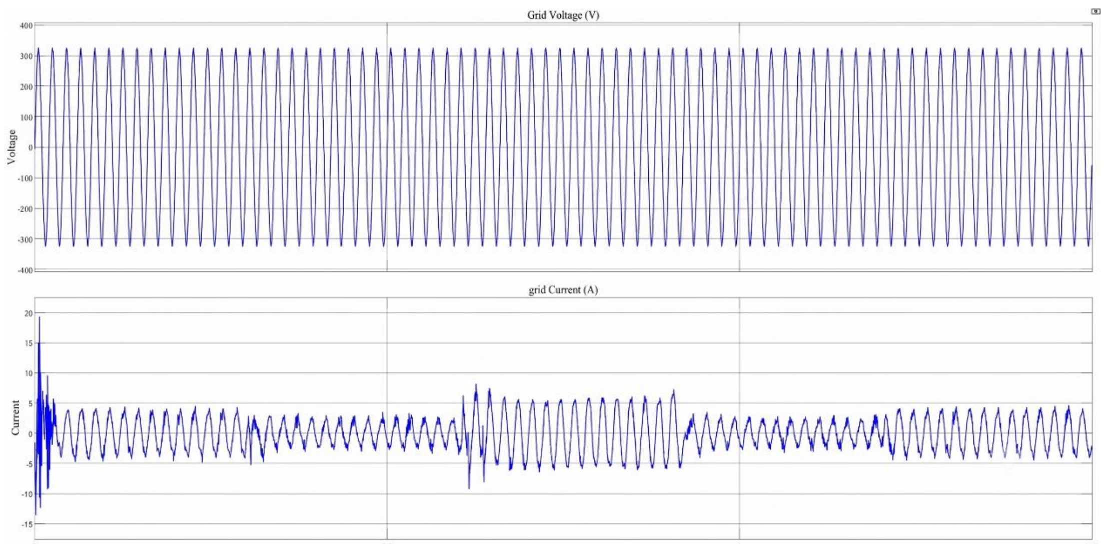

Fig. 15 Network characteristics (V, I)

6. Conclusion

The findings show very high accuracy, with small errors and correlation values close to one ($R \approx 0.99739$), which shows the model's capability. The validation examination included the evaluation of the minimum, maximum and median error, together with the study of the error distribution using histograms. This showed that there were low dispersion and a significant concentration around zero. Likewise, the training performance evidenced adequate stability and convergence of the model. In general terms, the results show that the proposed neural network is a robust and effective tool for the calculation of reference current, which enables its use in intelligent energy management systems in distributed generation scenarios. The validation study corroborated that the model has a good generalizability, due to the consistency between the errors of the training, validation and test sets. The fact that the error distribution is zero-centered and has low dispersion suggests that there is no significant bias, which strengthens the robustness of the model under various operating conditions of the energy system. In addition, the behavior of the training process evidenced a firm convergence towards a minimum of the error function, which ensures the effectiveness of the optimization algorithm used. With the Levenberg-Marquardt method, rapid convergence and appropriate tuning of neural network parameters was achieved, which prevented problems related to overfitting. The main contribution of this research is not the proposal of a new artificial neural network architecture, but the integration of a computationally efficient feedforward ANN into a complete energy management framework for a grid-connected photovoltaic system with battery storage. Compared with previous ANN-based studies, the proposed model focuses on direct estimation of the reference current required by the energy management strategy, providing high prediction accuracy while maintaining a relatively simple implementation suitable for real-time applications. Finally, the proposed model is a feasible option for its incorporation into energy management systems based on artificial intelligence, which makes it possible to optimize decision-making in photovoltaic systems with storage. As future work, it is suggested to validate the model with real data and to examine more sophisticated architectures that make it possible to further increase the adaptability and accuracy of the system.

Conflicts of Interest

The authors declare that there is no conflict of interest.

Funding Statement

Not Applicable.

References

[1] Sadegh Motahar, and Hamed Bagheri-Esfeh, "Artificial Neural Network-based Assessment of Grid-Connected Photovoltaic Thermal Systems in Heating Dominated Regions of Iran," *Sustainable Energy Technologies and Assessments*, vol. 39, 2020. [CrossRef] [Google Scholar] [Publisher Link]

[2] A. Rajabi et al., "Innovative Approaches for Assessing and Enhancing the Hosting Capacity of PV-rich Distribution Networks: An Australian Perspective," *Renewable and Sustainable Energy Reviews*, vol. 161, 2022. [CrossRef] [Google Scholar] [Publisher Link]

[3] Ezzitouni Jarmouni et al., "Energy Management in Connected and Disconnected mode of a Photovoltaic System with a Battery Storage using an Artificial Neural Network Technique," *Indonesian Journal of Electrical Engineering and Computer Science*, vol. 23, no. 1, pp. 54-62, 2021. [Google Scholar]

[4] Collins Ngong Sang et al., "Optimizing Photovoltaic Grid-Connected Power Systems Through Artificial Intelligence and Robust Nonlinear Control," *Engineering Reports*, vol. 7, no. 7, pp. 1-22, 2025. [CrossRef] [Google Scholar] [Publisher Link]

[5] Karim El Mezdi et al., "Nonlinear Control Design and Stability Analysis of Hybrid Grid-Connected Photovoltaic-Battery Energy Storage System with ANN-MPPT Method," *Journal of Energy Storage*, vol. 72, 2023. [CrossRef] [Google Scholar] [Publisher Link]

[6] Muhammad Shoaib Bhutta et al., "Optimizing Solar Power Efficiency in Smart Grids using Hybrid Machine Learning Models for Accurate Energy Generation Prediction," *Scientific Reports*, vol. 14, no. 1, pp. 1-25, 2024. [CrossRef] [Google Scholar] [Publisher Link]

[7] El-Khatib, Mohamed Fawzy, and Elsayed Atif Aner, "Efficient MPPT Control for a Photovoltaic System using Artificial Neural Networks," *ERU Research Journal*, vol. 2, no. 3, pp. 358-398, 2023. [Google Scholar]

[8] Pavitra Shukl, and Bhim Singh, "Delta-Bar-Delta Neural-Network-based Control Approach for Power Quality Improvement of Solar-PV-Interfaced Distribution System," *IEEE Transactions on Industrial Informatics*, vol. 16, no. 2, pp. 790-801, 2020. [CrossRef] [Google Scholar] [Publisher Link]

[9] M. Joly et al., "Novel Control Strategy based Energy Management in Renewable Energy in Grid Connected System," *Optimal Control Applications and Methods*, vol. 46, no. 6, pp. 2423-2437, 2025. [CrossRef] [Google Scholar] [Publisher Link]

[10] S. Boualem et al., "Power Management Strategy based on Elman Neural Network for Grid-Connected Photovoltaic-Wind-Battery Hybrid System," *Computers and Electrical Engineering*, vol. 99, 2022. [CrossRef] [Google Scholar] [Publisher Link]

[11] Ravichandran Balakrishnan et al., "Reduction in Residential Electricity Bill and Carbon Dioxide Emission through Renewable Energy Integration using an Adaptive Feed-Forward Neural Network System and MPPT Technique," *Sustainability*, vol. 15, no. 19, pp. 1-25, 2025. [CrossRef] [Google Scholar] [Publisher Link]

[12] Prashant Nene, and Dolly Thankachan, "Design of an Intelligent AI-based Multi-Layer Optimization Framework for Grid-Tied Solar PV-Fuel Cell Hybrid Energy Systems," *MethodsX*, vol. 15, pp. 1-17, 2025. [CrossRef] [Google Scholar] [Publisher Link]

[13] Ibrahim Alsaidan et al., "An Intelligent Approach to Active and Reactive Power Control in a Grid-Connected Solar Photovoltaic System," *Sustainability*, vol. 13, no. 8, pp. 1-24, 2021. [CrossRef] [Google Scholar] [Publisher Link]

[14] Amir Miraki, Pekka Parviainen, and Reza Arghandeh, "Electricity Demand Forecasting at Distribution and Household Levels using Explainable Causal Graph Neural Network," *Energy and AI*, vol. 16, pp. 1-11, 2024. [CrossRef] [Google Scholar] [Publisher Link]

[15] Yang Sun et al., "Artificial Neural Network for Control and Grid Integration of Residential Solar Photovoltaic Systems," *IEEE Transactions on Sustainable Energy*, vol. 8, no. 4, pp. 1484-1495, 2017. [CrossRef] [Google Scholar] [Publisher Link]

[16] Satyajeet Sahoo et al., "Artificial Deep Neural Network in Hybrid PV System for Controlling the Power Management," *International Journal of Photoenergy*, vol. 2022, no. 1, pp. 1-12, 2022. [CrossRef] [Google Scholar] [Publisher Link]

[17] Zhiming Gu et al., "Optimizing Photovoltaic Integration in Grid Management via a Deep Learning-based Scenario Analysis," *Scientific Reports*, vol. 15, no. 1, pp. 1-18, 2025. [CrossRef] [Google Scholar] [Publisher Link]

[18] Ossama Dankar et al., "A Neural Network-based Model Predictive Control for a Grid-Connected Photovoltaic-Battery System with Vehicle-to-Grid and Grid-to-Vehicle Operations," *Electricity*, vol. 6, no. 2, pp. 1-31, 2025. [CrossRef] [Google Scholar] [Publisher Link]

[19] Saad A. Mohamed Abdelwahab et al., "Comparative Analysis of Reinforcement Learning and Artificial Neural Networks for Inverter Control in Improving the Performance of Grid-Connected Photovoltaic Systems," *Scientific Reports*, vol. 15, no. 1, pp. 1-24, 2025. [CrossRef] [Google Scholar] [Publisher Link]

[20] Ruben Rafael Boros, Marcell Jobbágy and István Bodnár, "Optimized Real-Time Energy Management and Neural Network-based Control for Photovoltaic-Integrated Hybrid Uninterruptible Power Supply Systems," *Energies*, vol. 18, no. 6, pp. 1-32, 2025. [CrossRef] [Google Scholar] [Publisher Link]

[21] Chun Wu et al., "Optimal Energy Management for Prosumers and Power Plants Considering Transmission Congestion based on Carbon Emission Flow," *Applied Energy*, vol. 377, 2025. [CrossRef] [Google Scholar] [Publisher Link]

[22] Lakhdar Nadjib Boucetta et al., "Enhanced Forecasting Accuracy of a Grid-Connected Photovoltaic Power Plant: A Novel Approach using Hybrid Variational Mode Decomposition and a CNN-LSTM Model," *Energies*, vol. 17, no. 7, pp. 1-21, 2024. [CrossRef] [Google Scholar] [Publisher Link]

[23] Florus Härtel, and Thilo Bocklisch, "Minimizing Energy Cost in PV Battery Storage Systems using Reinforcement Learning," *IEEE Access*, vol. 11, pp. 39855-39865, 2023. [CrossRef] [Google Scholar] [Publisher Link]

[24] A. Mellit, A. Massi Pavan, and V. Lughi, "Deep Learning Neural Networks for Short-Term Photovoltaic Power Forecasting," *Renewable Energy*, vol. 172, pp. 276-288, 2021. [CrossRef] [Google Scholar] [Publisher Link]

[25] Prabhat Ranjan Bana, Simone Vanti, and Mohammad Amin, "Single-Stage Grid-Connected PV System with Artificial Neural Network Controller," *2021 IEEE 22nd Workshop on Control and Modelling of Power Electronics (COMPEL)*, Cartagena, Colombia, pp. 1-7, 2021. [CrossRef] [Google Scholar] [Publisher Link]

[26] N. Rathika et al., "Seagull-Optimized Artificial Neural Network-based Innovative Energy Management System using Improvised Boost Converter and Coupled Inductor," *Electrical Engineering*, vol. 107, no. 4, pp. 5207-5230, 2025. [CrossRef] [Google Scholar] [Publisher Link]

[27] Mithul Raaj A.T et al., "Intelligent Energy Management Across Smart Grids Deploying 6G IoT, AI, and Blockchain in Sustainable Smart Cities," *IoT*, vol. 5, no. 3, pp. 560-591, 2024. [CrossRef] [Google Scholar] [Publisher Link]

[28] Chabakata Mahamat, Jessica Bechet, and Laurent Linguet, "Artificial Neural Network Control Applied to a Photovoltaic-Battery Microgrid System," *AI, Computer Science and Robotics Technology*, vol. 3, no. 1, pp. 1-20, 2024. [CrossRef] [Google Scholar] [Publisher Link]

[29] Dácil Díaz-Bello et al., "Optimizing Photovoltaic Power Plant Forecasting with Dynamic Neural Network Structure Refinement," *Scientific Reports*, vol. 15, no. 1, pp. 1-29, 2025. [CrossRef] [Google Scholar] [Publisher Link]

[30] Hongyang Zhang, and Tiechao Wang, "Adaptive Neural Network Dynamic Surface Optimal Saturation Control for Single-Phase Grid-Connected Photovoltaic Systems," *Optimal Control Applications and Methods*, vol. 46, no. 1, pp. 174-196, 2025. [CrossRef] [Google Scholar] [Publisher Link]

[31] Fernanda Remache et al., "Simulation of Hybrid PV Solar System with Fuel Cell in MATLAB Simulink," *WSEAS Transactions on Circuits and Systems*, vol. 23, pp. 172-183, 2024. [Google Scholar]

[32] Benchikh Salma et al., "Improving Photovoltaic System Performance with Artificial Neural Network Control," *Data and Metadata*, vol. 2, no. 144, pp. 1-10, 2023. [Google Scholar]

[33] Anil Kumar, Prianka Chaudhary, and Owais Ahmad Shah, "Intelligent Controller based on Artificial Neural Network and INC based MPPT for Grid Integrated Solar PV System," *International Journal of Robotics and Control Systems*, vol. 3, no. 4, pp. 839-852, 2023. [CrossRef] [Google Scholar] [Publisher Link]

[34] Salah Mahdi Thajeel and Doğu Çağdaş Atilla, "Reinforcement Neural Network-based Grid-Integrated PV Control and Battery Management System," *Energies*, vol. 18, no. 3, pp. 1-20, 2025. [CrossRef] [Google Scholar] [Publisher Link]

[35] Joffre R. Constante et al., "Adversarial Learning as a PMU Signal Filtering Technique in Load Models Identification," *IEEE Access*, vol. 13, pp. 100601-100613, 2025. [CrossRef] [Google Scholar] [Publisher Link]